Brief Communication

Bioaccumulation of microplastics in decedent human brains

Alexander J. Nihart [1,12], Marcus A. Garcia[1,12], Eliane El Hayek [1,12], Rui Liu[1], Marian Olewine[1], Josiah D. Kingston[1], Eliseo F. Castillo[2], Rama R. Gullapalli[3], Tamara Howard[4], Barry Bleske[5], Justin Scott [6], Jorge Gonzalez-Estrella [6], Jessica M. Gross [7], Michael Spilde[8], Natalie L. Adolphi[9], Daniel F. Gallego[9], Heather S. Jarrell[9], Gabrielle Dvorscak[9], Maria E. Zuluaga-Ruiz[10], Andrew B. West [11] & Matthew J. Campen [1] ✉

Rising global concentrations of environmental microplastics and nanoplastics (MNPs) drive concerns for human exposure and health outcomes. Complementary methods for the robust detection of tissue MNPs, including pyrolysis gas chromatography–mass spectrometry, attenuated total reflectance–Fourier transform infrared spectroscopy and electron microscopy with energy-dispersive spectroscopy, confirm the presence of MNPs in human kidney, liver and brain. MNPs in these organs primarily consist of polyethylene, with lesser but significant concentrations of other polymers. Brain tissues harbor higher proportions of polyethylene compared to the composition of the plastics in liver or kidney, and electron microscopy verified the nature of the isolated brain MNPs, which present largely as nanoscale shard-like fragments. Plastic concentrations in these decedent tissues were not influenced by age, sex, race/ethnicity or cause of death; the time of death (2016 versus 2024) was a significant factor, with increasing MNP concentrations over time in both liver and brain samples ($P = 0.01$). Finally, even greater accumulation of MNPs was observed in a cohort of decedent brains with documented dementia diagnosis, with notable deposition in cerebrovascular walls and immune cells. These results highlight a critical need to better understand the routes of exposure, uptake and clearance pathways and potential health consequences of plastics in human tissues, particularly in the brain.

Environmental concentrations of anthropogenic microplastic and nanoplastic (MNP), polymer-based particulates ranging from 500 μm in diameter down to 1 nm, have increased exponentially over the past half century[1,2]. The extent to which MNPs cause human harm or toxicity is unclear, although recent studies associated MNP presence in carotid atheromas with increased inflammation and risk of future adverse cardiovascular events[3,4]. In controlled cell culture and animal exposure studies, MNPs exacerbate disease or drive toxic outcomes, but at concentrations with unclear relevance to human exposures and body burdens[5,6]. The mantra of the field of toxicology–'dose makes the poison' (Paracelsus)–renders such discoveries as easily anticipated; what is not clearly understood is the tissue distribution and internal dose of MNPs in humans, which confounds our ability to interpret the controlled exposure study results.

So far, visual microscopic spectroscopy methods have identified particulates in organs, such as the lungs, intestine[7] and placenta[8]. These methods are often limited to larger (>5 μm) particulates; thus, smaller nanoplastics are unintentionally excluded. As a new approach,
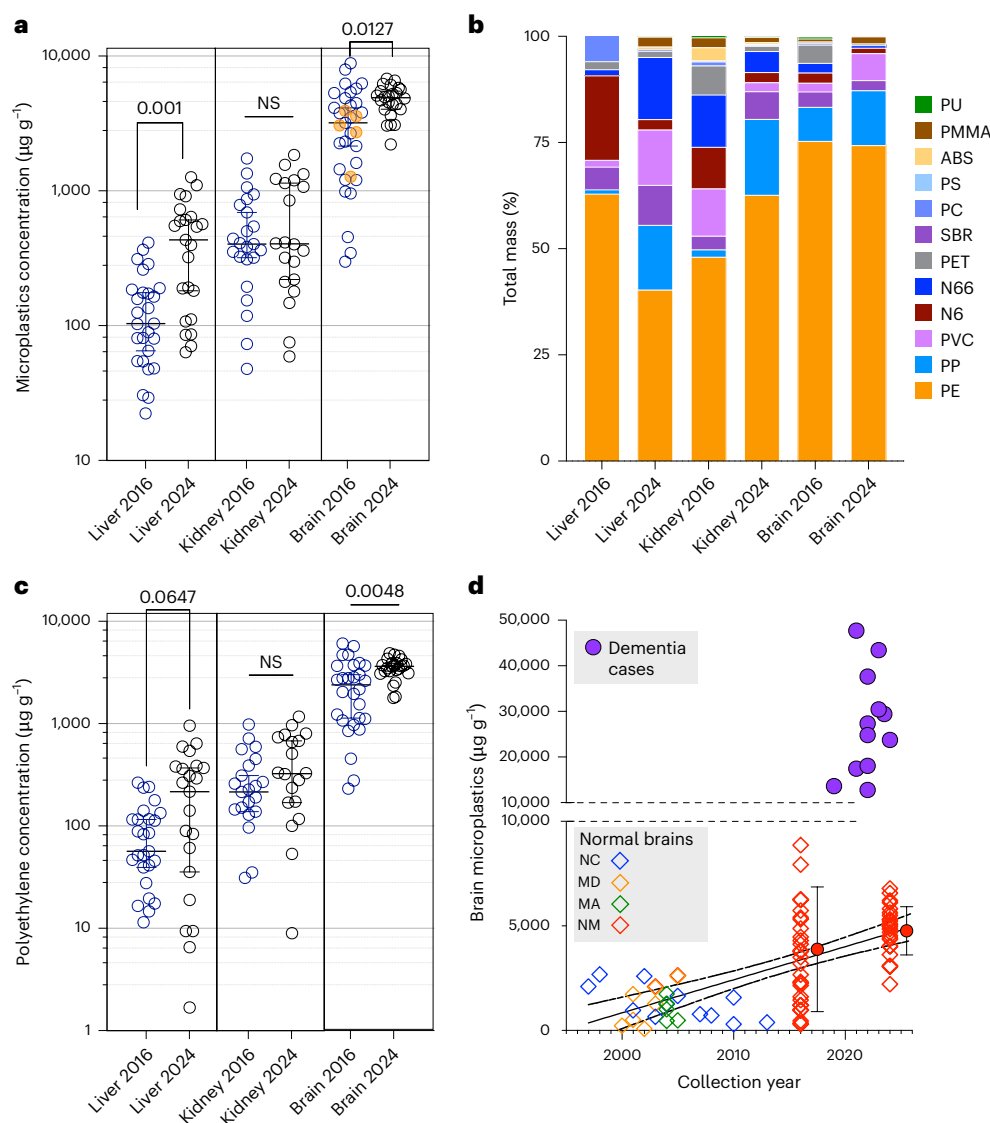
Fig. 1 | Overview of total MNP concentrations from all decedent samples from liver, kidney and brain. a, Microplastic concentrations in liver, kidney and brain decedent human samples (n = 20–28 separate participants for each timepoint; Supplementary Table 1) from the UNM OMI. Data are shown on a $\log_{10}$ scale, with the bar representing the group median value and 95% confidence interval. Orange-colored symbols in the 2016 brain samples were analyzed independently at Oklahoma State University. P values from Mann–Whitney tests (two-sided) indicate significant differences in samples from the same organ between 2016 and 2024 (with more comprehensive statistical treatments in Supplementary Methods–Statistical analysis). Brain MNP concentrations were significantly higher than liver and kidney, analyzed by two-way ANOVA (P < 0.0001). **b**, Overall distribution of 12 different polymers suggests a greater accumulation of PE in the brain relative to liver or kidney (average shown per group; see Extended Data Fig. 1 for individual data). **c**, PE (which was in the highest abundance and consistently had the highest confidence spectra) concentrations in all organs followed similar trends compared to total plastics (also represented as group median value and

95% confidence interval; two-sided Mann–Whitney test). **d**, Additional brain samples from specimens collected from 1997 to 2013 were obtained from the Duke Kathleen Price Bryan Brain Bank in North Carolina (n = 13, blue diamonds; NC), the Harvard Brain Tissue Resource Center in Massachusetts (n = 9, green diamonds; MA) and the National Institute of Child Health and Human Development Brain and Tissue Bank at the University of Maryland (n = 5, orange diamonds; MD) show lower concentrations of microplastics. Brain samples from decedents with diagnosed dementia (n = 12, purple circles) from UNM exhibit far greater MNP concentrations than brain tissues from participants without dementia from New Mexico (red thin-outline diamonds; NM). Overall linear regression trend was significantly nonzero (P < 0.0001) with an R^2 = 0.3982; summary points for 2016 and 2024 normal UNM OMI brains reflect mean ± s.d. N66, nylon 66; ABS, acrylonitrile butadiene styrene; PET, polyethylene terephthalate; N6, nylon-6; PMMA, poly(methyl methacrylate); PU, polyurethane; PC, polycarbonate; PS, polystyrene.

pyrolysis gas chromatography–mass spectrometry (Py-GC/MS) has been applied to blood[9], placentas[10] and recently major blood vessels[3,4] in a manner that appears more cumulative, quantitative and less biased when coupled with orthogonal methods. Py-GC/MS data between labs has been comparable, providing confidence in this method for human tissue analysis[3,9,10]. Here we applied Py-GC/MS in concert with visualization methods to assess the relative distribution of MNPs in major organ systems from human decedent livers, kidneys and brains.

Results and discussion

We obtained de-identified, postmortem human liver (right central parenchyma), kidney (wedge piece containing cortex and medulla) and brain (frontal cortex) samples, retrospectively from 2016 and 2024 autopsy specimens (Supplementary Table 1), in cooperation with and approval from the University of New Mexico (UNM) Office of the Medical Investigator (OMI) in Albuquerque, New Mexico (NM), under the guidance of a trained forensic pathologist (D.F.G.) who selected consistent regions

from all organs. Py-GC/MS measurements of MNP concentrations in decedent liver and kidney specimens were similar, with the median value of total plastics at 433 and 404 µg g^{-1}, respectively, from 2024 samples (Fig. 1a and Supplementary Table 1). These were higher than previously published data for human placentas (median = 63.4 µg g^{-1})[10] and testes (median = 299 µg g^{-1})[11]. Brain samples, all derived from the frontal cortex, exhibited substantially higher concentrations of MNPs than liver or kidney (two-way analysis of variance (ANOVA), $P < 0.0001$), but comparable to recently published Py-GC/MS data from carotid plaques[4], with a median of 3345 µg g^{-1} (25–75%: 1,267–5,213 µg g^{-1}) in 2016 samples and 4917 µg g^{-1} (25–75%: 4,026–5,608 µg g^{-1}) in 2024 samples (Fig. 1a and Supplementary Table 1).

Liver and brain samples from 2024 had significantly higher concentrations of MNPs than 2016 samples on both post hoc multiple comparisons of the two-way ANOVA (Supplementary Tables 4–7 and Supplementary Fig. 6), consistent with results from a multiple regression analysis of brain concentrations considering the potential influence of other demographic variables (Supplementary Tables 8–10). Five brain samples from 2016 (highlighted in orange in Fig. 1a) were analyzed independently by colleagues at Oklahoma State University using Py-GC/MS, and those values were consistent with our findings ($P = 0.49$ for a Student's t test comparing UNM and OSU data). The proportion of polyethylene (PE) in the brain (75% on average) was greater relative to other polymers and compared to PE in the liver and kidney ($P < 0.0001$; Fig. 1b and Extended Data Fig. 1). PE, polypropylene (PP), polyvinyl chloride (PVC) and styrene-butadiene rubber (SBR) concentrations specifically increased from 2016 to 2024 in liver and brain samples (Fig. 1c and Extended Data Fig. 2). PE predominance was confirmed with attenuated total reflectance–Fourier transform infrared spectroscopic analysis from five brain samples, although other polymers were not as consistent in prevalence, possibly due to differences in prevalence across size distributions and limited sampling (Supplementary Tables 9–13 and Supplementary Figs. 17–25).

To expand these findings, we obtained brain tissue from earlier time frames (1997–2013) with a mean age of death comparable to the NM cohorts (52.8 ± 34.3 years) from locations in the eastern United States, along with samples from a repository of dementia cases at UNM. Py-GC/MS analysis revealed lower overall MNP concentrations in East Coast samples (median = 1,254 µg g^{-1}; Supplementary Table 1 and Fig. 1d). While geographical differences cannot be ruled out, we applied a simple linear regression including all normal brain biospecimen data, which revealed significantly increasing trends for total plastics, PE, PP, PVC and SBR (Extended Data Fig. 2). To extend findings to a specific neurological condition, Py-GC/MS was conducted on 12 dementia cases collected in the NM OMI. These cases included Alzheimer's disease ($n = 6$), vascular dementia ($n = 3$) and other dementia ($n = 3$) specimens from 2019 to 2024. Py-GC/MS analysis revealed total plastics concentrations in dementia samples (median = 26,076 µg g^{-1}; Fig. 1d and Supplementary Table 1) that were higher than in any normal frontal cortex cohort ($P < 0.0001$ by two-sided t test). Atrophy of brain tissue, impaired blood–brain barrier integrity and poor clearance mechanisms are hallmarks of dementia and would be anticipated to increase MNP concentrations; thus, no causality is assumed from these findings.

Using scanning electron microscopy (SEM) and polarization wave microscopy, refractory inclusions were identified in all organs histologically (Fig. 2, Extended Data Fig. 3 and Supplementary Figs. 7–16). Within the liver, these inclusions were widely dispersed but also notably aggregated within acellular regions consistent with the expected frequency and morphology of lipid droplets, with rod-shaped particles in the 1–5 µm size range (Extended Data Fig. 3a). In the kidney, an elevated presence of refractile inclusions of similar sizes was noted in glomeruli and along tubules (Extended Data Fig. 3a–d). Based on elevated concentrations of polymers identified by Py-GC/MS in these tissues, we suspected that much of the MNPs may be present in the nanoscale range, too small for visualization by light microscopy. Transmission

electron microscopy (TEM) was therefore conducted on the dispersed KOH-insoluble pellets obtained from the liver and kidney (Extended Data Fig. 3e,f and Supplementary Fig. 9). While this visualization method cannot provide spectroscopic confirmation of polymer composition, we observed common shapes and sizes across samples and tissue types. Particulates isolated from the pellets and well-dispersed appeared shard-like and were typically less than 0.4 µm in length, consistent with recent findings of nanoplastics in farmed mussels[12]. SEM with energy-dispersive spectroscopy confirmed that particles observed in livers, kidneys and brains were principally composed of carbon (Extended Data Figs. 4–7). Based on the larger morphology of particulates observed in situ versus those isolated and dispersed from the pellets of digested tissue, we postulate that aggregation of nanoplastics may occur in the liver and kidney.

In brain tissues, larger (1–5 µm) refractile inclusions were not seen, but smaller particulates (<1 µm) were noted in the brain parenchyma (Fig. 2a–c and Supplementary Figs. 10–15). Given the resolution limitations of light microscopy, we examined resuspended brain pellets by TEM, which revealed largely 100–200 nm long shards or flakes (Fig. 2d and Supplementary Figs. 9 and 16). In situ, we confirmed that particles found in the brain were carbon-based by SEM with energy-dispersive X-ray spectrometry (EDS; Extended Data Figs. 6 and 7). In dementia samples, many refractile inclusions were prominent in regions with inflammatory cells and along the vascular wall (Fig. 2e,f). MNP uptake and distribution pathways are poorly understood, and the mechanism of how nanoplastics are delivered to and taken up into the brain is unknown. Insights from *Daphnia magna* suggest clathrin-dependent endocytosis and macropinocytosis may underlie nanoplastic translocation within the intestine[13]; we posit a similar uptake may occur in human ingestion of lipids that would also facilitate selective transfer into the brain. While blood was not cleared from the decedent's organs during autopsy, it is unlikely that the nanoplastics in the brain are selectively contained in the vascular compartment, as the kidneys and livers would also have comparable blood volumes.

While we suspected that MNPs might accumulate in the body over a lifespan, the lack of correlation between total plastics and decedent age ($P = 0.87$ for brain data) does not support this (Supplementary Fig. 1). However, total mass concentration of plastics in the brains analyzed in this study increased by approximately 50% in the past 8 years. Thus, we postulate that the exponentially increasing environmental concentrations of MNPs[2,14] may analogously increase internal maximal concentrations. Although there are few studies to draw on yet performed in mammals, in zebrafish exposed to constant concentrations, nanoplastic uptake increased to a stable plateau and cleared after exposure[15]; however, the maximal internal concentrations were increased proportionally with higher nanoplastic exposure concentrations. While clearance rates and elimination routes of MNPs from the brain remain uncharacterized, it is possible that an equilibrium—albeit variable between people—might occur between exposure, uptake and clearance, with environmental exposure concentrations ultimately determining the internal body burden.

Although the current data derive from multiple tissue banks and two analytic sites replicating key results, the new analytical Py-GC/MS methods applied here are yet to be widely adopted and refined into standardized tests for clinical specimens. Both analytical laboratories (UNM and OSU) observed a ~25% within-sample coefficient of variation, which does not alter the conclusions regarding temporal trends or accumulation in brains relative to other tissues, given the magnitude of those effects. Numerous quality control steps ensure that external contaminants are not impacting the results, including Py-GC/MS assessment of KOH and formalin storage control sample 'blanks' and measurements of the polymer composition of all plastic tubes and pipette tips that are essential in the digestion and measurement process (Supplementary Figs. 2–4). Decedent specimen collections over the past 30 years were not focused on minimizing external plastic
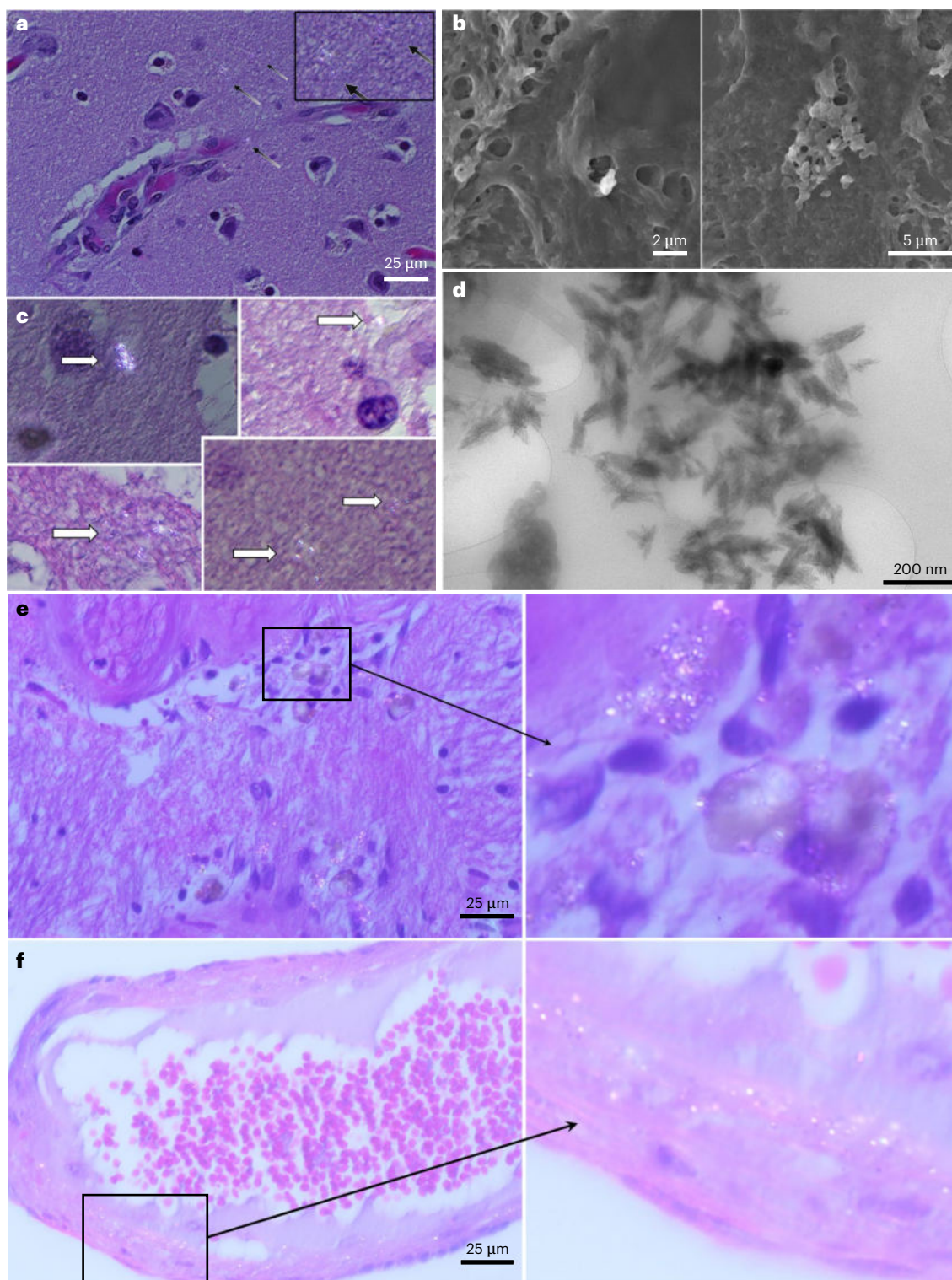
Fig. 2 | Visualization of putative plastics in the brain. a,b, Polarization wave microscopy (**a**, black arrows indicate refractory inclusions; inset is a digital magnification for clarity) and SEM (**b**, visual fields are 15.4 and 20.1 μm wide) were used to scan sections of brain from decedent human samples. **c,** Large (>1 μm) inclusions were not observed; additional polarization wave examples are highlighted (white arrows highlight submicron refractory inclusions). Resolution limitations of these technologies drove the use of TEM to examine the extracts from the pellets used for Py-GC/MS. **d,** Example TEM images resolved innumerable shard- or flake-like solid particulates following dispersion, with dimensions largely <200 nm in length and <40 nm in width. **e,f,** Polarization wave microscopy reveals substantially more refractile inclusions in dementia cases, especially in regions with associated immune cell accumulation (**e**) and along the vascular walls (**f**). All images were collected on a small subset of participants (n = 10 for normal brains; n = 3 for dementia cases) to provide visual evidence to support analytical chemistry.

contamination. However, given the consistent nature of handling and processing across all organ samples within objectively clean clinical and forensic settings, the significant accumulation of MNPs in the brain cannot be dismissed as an artifact of contamination. Furthermore, the 2016 samples were stored for 84–96 months compared to only 2–4 months for the 2024 samples, which exhibited greater concentrations of polymer. Thus, contamination from plastic storage vessels should not influence the conclusions. For the brain, especially, greater attention to anatomical features, such as white versus gray matter, vascularization and glia content, should be carefully evaluated in future studies to reduce variation. Finally, by obtaining only a single sample from each organ for each participant, distribution heterogeneity within tissues remains uncharacterized.

Our estimates of polymer mass concentration could be impacted by several factors that may lead to overestimation or underestimation. The KOH digestion extensively eliminated biological material from the pellets through saponification of triglycerides and denaturing of proteins (Supplementary Fig. 5). However, the final pellets still contained unknown residual biomatrix, which could present challenges for mass spectral interference. KOH reduced the liver and kidney mass by 99.4%, while the brain samples were reduced by 91.8%, that is, the resultant average pellet mass derived from 500 mg of starting material was approximately 3 mg and 41 mg, respectively. This discrepancy is proportional to, and consistent with, the mass of the polymer measured. However, unknown organic molecules likely remain and influence the resultant Py-GC/MS spectra. Lipids have been noted as a potential source of interference in Py-GC/MS analysis of PE[16]. Our method of KOH digestion and physical separation of solids was designed to reduce this concern, rather than augment it with a liquid–liquid extraction in organic solvents that would selectively drive lipid partitioning. Furthermore, the spectra suggest a reduction of longer carbon chains in the pyrolysis chromatogram, which is potentially due to advanced oxidative degradation of the MNPs and excess carbonyl formation that may lead to an underestimation of the concentration, as our standards are created with pristine polymers[17,18]. Finally, given the observed small size of nanoscale particles isolated from the human specimens (typically <200 nm in length), it is likely that ultracentrifugation incompletely collected nanoplastics in the analytical samples, also contributing to potential underestimation. The shape and size of observed nanoparticles in the isolated material from human specimens taxes the limits of modern analytical instrumentation but may reflect an end-stage product of plastic degradation that is uniquely suited for human uptake and accumulation.

Conclusions

The present data suggest a trend of increasing MNP concentrations in the brain and liver. The majority of MNPs found in tissues consist of PE and appear to be nanoplastic shards or flakes. MNP concentrations in normal decedent brain samples were 7–30 times greater than the concentrations seen in livers or kidneys, and brain samples from dementia cases exhibited even greater MNP presence. These data are associative and do not establish a causal role for such particles affecting health. For this, refinements to the analytical techniques, more complex study designs and much larger cohorts are needed. Given the exponentially rising environmental presence of MNPs[19–21], these data compel a much larger effort to understand whether MNPs have a role in neurological disorders or other human health effects.

Online content

Any methods, additional references, Nature Portfolio reporting summaries, source data, extended data, supplementary information, acknowledgements, peer review information; details of author contributions and competing interests; and statements of data and code availability are available at https://doi.org/10.1038/s41591-024-03453-1.

References

1. Thompson, R. C. et al. Lost at sea: where is all the plastic? *Science* **304**, 838 (2004).
2. Stubbins, A., Law, K. L., Munoz, S. E., Bianchi, T. S. & Zhu, L. Plastics in the Earth system. *Science* **373**, 51–55 (2021).
3. Liu, S. et al. Microplastics in three types of human arteries detected by pyrolysis-gas chromatography/mass spectrometry (Py-GC/MS). *J. Hazard. Mater.* **469**, 133855 (2024).
4. Marfella, R. et al. Microplastics and nanoplastics in atheromas and cardiovascular events. *N. Engl. J. Med.* **390**, 900–910 (2024).
5. Dong, C. D. et al. Polystyrene microplastic particles: in vitro pulmonary toxicity assessment. *J. Hazard. Mater.* **385**, 121575 (2020).
6. Dibbon, K. C. et al. Polystyrene micro- and nanoplastics cause placental dysfunction in mice. *Biol. Reprod.* **110**, 211–218 (2023).
7. Zhu, L. et al. Tissue accumulation of microplastics and potential health risks in human. *Sci. Total Environ.* **915**, 170004 (2024).
8. Ragusa, A. et al. Plasticenta: first evidence of microplastics in human placenta. *Environ. Int.* **146**, 106274 (2021).
9. Leslie, H. A. et al. Discovery and quantification of plastic particle pollution in human blood. *Environ. Int.* **163**, 107199 (2022).
10. Garcia, M. A. et al. Quantitation and identification of microplastics accumulation in human placental specimens using pyrolysis gas chromatography mass spectrometry. *Toxicol. Sci.* **199**, 81–88 (2024).
11. Hu, C. et al. Microplastic presence in dog and human testis and its potential association with sperm count. *Toxicol. Sci.* **200**, 235–240 (2024).
12. Fraissinet, S., De Benedetto, G. E., Malitesta, C., Holzinger, R. & Materić, D. Microplastics and nanoplastics size distribution in farmed mussel tissues. *Commun. Earth Environ.* **5**, 128 (2024).
13. Das, A., Terry, L. R., Sanders, S., Yang, L. & Guo, H. Confocal surface-enhanced raman imaging of the intestinal barrier crossing behavior of model nanoplastics in *Daphnia magna*. *Environ. Sci. Technol.* **58**, 11615–11624 (2024).
14. Landrigan, P. J. Plastics, fossil carbon, and the heart. *N. Engl. J. Med.* **390**, 948–950 (2024).
15. Habumugisha, T., Zhang, Z., Fang, C., Yan, C. & Zhang, X. Uptake, bioaccumulation, biodistribution and depuration of polystyrene nanoplastics in zebrafish (*Danio rerio*). *Sci. Total Environ.* **893**, 164840 (2023).
16. Rauert, C., Pan, Y., Okoffo, E. D., O'Brien, J. W. & Thomas, K. V. Extraction and pyrolysis-GC-MS analysis of polyethylene in samples with medium to high lipid content. *J. Environ. Expo. Assess.* **1**, 13 (2022).
17. Ainali, N. M., Bikiaris, D. N. & Lambropoulou, D. A. Aging effects on low- and high-density polyethylene, polypropylene and polystyrene under UV irradiation: an insight into decomposition mechanism by Py-GC/MS for microplastic analysis. *J. Anal. Appl. Pyrol.* **158**, 105207 (2021).
18. Toapanta, T. et al. Influence of surface oxidation on the quantification of polypropylene microplastics by pyrolysis gas chromatography mass spectrometry. *Sci. Total Environ.* **796**, 148835 (2021).
19. Wang, C. H., Zhao, J. & Xing, B. S. Environmental source, fate, and toxicity of microplastics. *J. Hazard. Mater.* **407**, 124357 (2021).
20. Geyer, R., Jambeck, J. R. & Law, K. L. Production, use, and fate of all plastics ever made. *Sci. Adv.* **3**, e1700782 (2017).
21. Landrigan, P. J. et al. The Minderoo-Monaco Commission on plastics and human health. *Ann. Glob. Health* **89**, 23 (2023).

[1]Department of Pharmaceutical Sciences, College of Pharmacy, University of New Mexico Health Sciences, Albuquerque, NM, USA. [2]Division of Gastroenterology and Hepatology, Department of Internal Medicine, University of New Mexico Health Sciences Center, Albuquerque, NM, USA. [3]Department of Pathology, University of New Mexico Health Sciences Center, Albuquerque, NM, USA. [4]Department of Cell Biology and Physiology, School of Medicine, University of New Mexico Health Sciences Center, Albuquerque, NM, USA. [5]Department of Pharmacy Practice and Administrative Sciences, College of Pharmacy, University of New Mexico Health Sciences Center, Albuquerque, NM, USA. [6]School of Civil & Environmental Engineering, Oklahoma State University, Stillwater, OK, USA. [7]Clinical and Translational Science Center, University of New Mexico Health Sciences Center, Albuquerque, NM, USA. [8]Department of Earth and Planetary Sciences, University of New Mexico, Albuquerque, NM, USA. [9]Office of the Medical Investigator, University of New Mexico, Albuquerque, NM, USA. [10]Grupo de Investigación en Rehabilitación de la Universidad del Valle (GIRUV), Cali, Colombia. [11]Duke Center for Neurodegeneration and Neurotherapeutics, Duke University, Durham, NC, USA. [12]These authors contributed equally: Alexander J. Nihart, Marcus A. Garcia, Eliane El Hayek. ✉e-mail: mcampen@salud.unm.edu